EFFECT OF DIFFERENT GEOMETRY FLOW PATTERN ON HEAT SINK PERFORMANCE

Fernando Cano-Banda, C. Ulises Gonzalez-Valle, Sindy Tarazona-Cardenas*, Abel Hernandez-Guerrero
Department of Mechanical Engineering,
University of Guanajuato,
Salamanca, Guanajuato,
Mexico,
E-mail: abel@ugto.mx

ABSTRACT

How to achieve appropriate operating temperatures in present-day electronic equipment is a matter of fervent discussion in the current technical literature. The highly demanding cooling requirements of these devices are a quite a challenging topic. In the present work some different non-conventional patterns for liquid cooled heat sinks are proposed. These new flow patterns distribute homogeneously the working fluid through the whole system promoting the enhanced of the heat sink performance and the uniformity temperature distribution at the base of the heat sink. These configurations consist of a flow inlet at the center of the heat sink (with the purpose of feeding the radial serpentine channels), and several flow outlets located on the outer side of the heat sink. Different cases are studied by varying the number of channels, channel length, and number of spirals used. Deionized water is selected as working fluid, considering in this study the dependence of fluid viscosity in regards with temperature, this parameter has shown to be crucial in thermal analysis of heat sinks. Each case studied shows a particular performance, thus, the pressure drop, the average temperature, the total dissipated energy, and other comparative parameters are reported to discuss advantages and disadvantages of every configuration.

INTRODUCTION

Nowadays, tendency of the actual processors and other electronic devices is to decrease its size and increase the total number of transistors on it; thus the heat rejection necessities are enlarged considerably. Due these important facts, ensuring high performance and efficiency of these systems is a big challenge. Liquid cooling technology has shown several advantages over the traditional methods using air, especially due to higher heat transfer coefficients that can be reached by liquid-cooling alternatives [1]. Tuckerman and Pease [2] proposed microchannels for cooling applications in the early 1980s; in this work a liquid cooled heat sink is studied, this device demonstrated high effectivity removing heat from a silicon chip. This heat sink was able to remove 790 W/cm^2, however, high pressure drop was also reported. In 2009 Xie et al. [3] corroborated the results obtained by Tuckerman and Pease and proved that it is possible to implement microchannels in liquid-cooled heat sinks. Xie et al. developed a numerical model that predicted the pressure drop and heat transfer presented in a microchannel heat sink obtaining promising results for this type of devices, with acceptable pressure drops.

Structures of natural systems, such as the circulatory system, have inspired some of the non-traditional geometries for micro-effective cooling devices. These patterns are known as branching networks and can help to reduce the flow resistance in flow networks decreasing the pressure drops presented by these devices. Yongping Ping Chen and Cheng [4] studied fractal-tree nets for cooling purposes on micro-electronic chips. The studied flow patter is rectangular and it is bifurcated in several levels. They observed that the new fractal net presented better heat transfer capabilities in comparison with well-worn configurations. In this study they also demonstrated that the overall pressure drop is reduced by the implementation of this type of patterns. Wang et al. [5] investigated similar models with a square heat sink; the results showed that tree-shaped geometries provides better temperature and fluid distribution reducing channel blockage. Similar non-traditional configurations have been analyzed and presented in several studies [6-8].

NOMENCLATURE

K	[W/m-K]	Thermal conductivity
c_p	[kJ/kg-K]	Specific heat
q''	[W/m^2]	Heat flux
$\dot{m}$	[kg/s]	Mass flow rate
R	[K/W]	Thermal resistance
T	[K]	Temperature
Δp	[kPa]	Pressure drop
$\dot{W}_p$	[W]	Pumping work
$\dot{\forall}$	[m^3/s]	Volumetric flow
u	[m/s]	Velocity component in x direction
v	[m/s]	Velocity component in y direction
w	[m/s]	Velocity component in z direction

Greek symbols

ρ	[kg/m^3]	Density
μ	[kg/m-s]	Dynamic viscosity

Subscript

b	Bottom
f	Fluid
Cu	Cooper
Ave	Average
In	Inlet
S	Surface
P	Pump

There are fewer studies employing minichannels on heat sinks. In 2013 Ho *et al.* [9] conducted an experimental research about the effect of using microencapsulated phase material (MEPCM) particles/water mixtures as coolant in the performance of a parallel rectangular minichannel heat sink. Jajja *et al.* [10] tested five different fin spacings in a minichannel heat sink for microprocessor cooling with water as working fluid. They concluded that geometrically enhanced

heat sinks have a lot of potential with common fluids a as water instead of non-common as nanofluids. On the other hand, Mu *et al.* [11] worked in a numerical study. The authors of this work analyzed the temperature uniformity on the heated surface of a novel minichannel heat sink. They tested four different distributor configurations with parallel rectangular minichannels. U-type, Z-type circulating type and tree-type were the channels configurations proved.

In the present work some non-traditional patterns for liquid-cooled heat sinks are proposed and studied. Radial serpentine flow patterns are studied varying the number of channels, channel length, and number of spirals. Variations of the velocity of the fluid at the inlet are studied and reported. Deionized water is used as working fluid. For each case effects of the pressure drop, temperature distribution, and thermal resistivity are reported.

GEOMETRY DESCRIPTION
The main purpose of this work is to analyze and compare the cooling performance, pressure drops, and temperature distribution of a square heat sink employing three designs with different non-traditional flow patterns. Figure 1a shows a schematic diagram of the computational domain implemented and the fluid inlet and outlets localization. Figure 1b presents the flow patterns configuration analyzed in this work. Three different non-traditional patterns are analyzed; each pattern presents variations in the number of channels as well as the inlets and outlets positions.

Three different squared cold plates of 49 mm lateral length were investigated. Symmetric boundary conditions were applied to the analyzed models; this implementation allows the reduction of the computational requirements of the models. Figure 2 presents the symmetrical regions of each design. Table 1 summarizes the different analyzed configurations.

Table 1. Proposed flow pattern configurations.

Configuration	Label	Number of flow outlets
1	D1	2
2	D2-A	4
3	D2-B	4

COMPUTATIONAL MODEL

Model Assumptions
The following assumptions are made in the developed numerical model in order reduce the model complexity increasing its accuracy.
(1) Steady state.
(2) Laminar and incompressible flow.
(3) Single phase flow.
(4) Negligible radiation heat transfer.
(5) Constant fluid properties excepting for the water viscosity.

Desionizated water was chosen as working fluid for the heat sink. Figure 1b shows the engraved flow pattern that represents the fluid domain, the white part represents the solid domain in the computational model studied in this work. Copper is chosen as the solid material which the heat sink is constructed of. The thermophysical properties of the selected materials are summarized in Table 2.

Table 2. Thermophysical properties of liquid desionizated water and copper.

Property	Value	Units
Water		
Viscosity, μ	$2.414\times10^{-5}(10^{247.8/(T-140)})$ [12]	kg/m-s
Thermal conductivity, k_f	0.6	W/m-K
Density, ρ_f	998.2	kg/m3
Specific heat, cp_f	4182	kJ/kg-K
Copper		
Thermal conductivity, k_{cu}	387.6	W/m-K
Density, ρ_{Cu}	8978	kg/m^3
Specific heat, c_{Cu}	381	kJ/kg-K

Governing equations
The main phenomena involved in the studied model can be described by the Equations 1-6. Equations 1-4 describe the fluid dynamics phenomenon which is coupled with Equation 5 which describes the presented heat transfers mechanisms.

$$\frac{\partial u}{\partial x} + \frac{\partial v}{\partial y} + \frac{\partial w}{\partial z} = 0 \tag{1}$$

$$\rho_f\left(u\frac{\partial u}{\partial x} + v\frac{\partial u}{\partial y} + w\frac{\partial u}{\partial z}\right) = -\frac{\partial p}{\partial x} + \nabla^2\mu u \tag{2}$$

$$\rho_f\left(u\frac{\partial v}{\partial x} + v\frac{\partial v}{\partial y} + w\frac{\partial v}{\partial z}\right) = -\frac{\partial p}{\partial y} + \nabla^2\mu v \tag{3}$$

$$\rho_f\left(u\frac{\partial w}{\partial x} + v\frac{\partial w}{\partial y} + w\frac{\partial w}{\partial z}\right) = -\frac{\partial p}{\partial z} + \nabla^2\mu w \tag{4}$$

Equation 5 is the energy equation applied to the fluid domain. As mentioned before, all properties are considered constants but the viscosity, this fact is shown in Equations 2-4.

$$\rho_f c_{pf}\left(u\frac{\partial T}{\partial x} + v\frac{\partial T}{\partial y} + w\frac{\partial T}{\partial z}\right) = k_f\nabla^2 T \tag{5}$$

The energy equation for the solid domain is described by Equation 6.

$$\left(\nabla^2 \cdot T\right) = 0 \tag{6}$$

An important comparison parameter in this type of analysis is the local thermal resistance. This parameter is defined as the temperature difference of the surface and fluid inlet dived by the total heat flow rejected by the base.

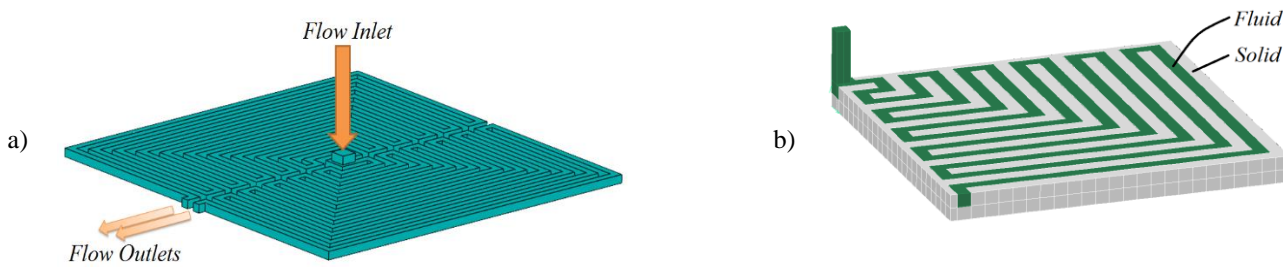$$R = \frac{T_s - T_{f,in}}{q'' A_s} \tag{7}$$

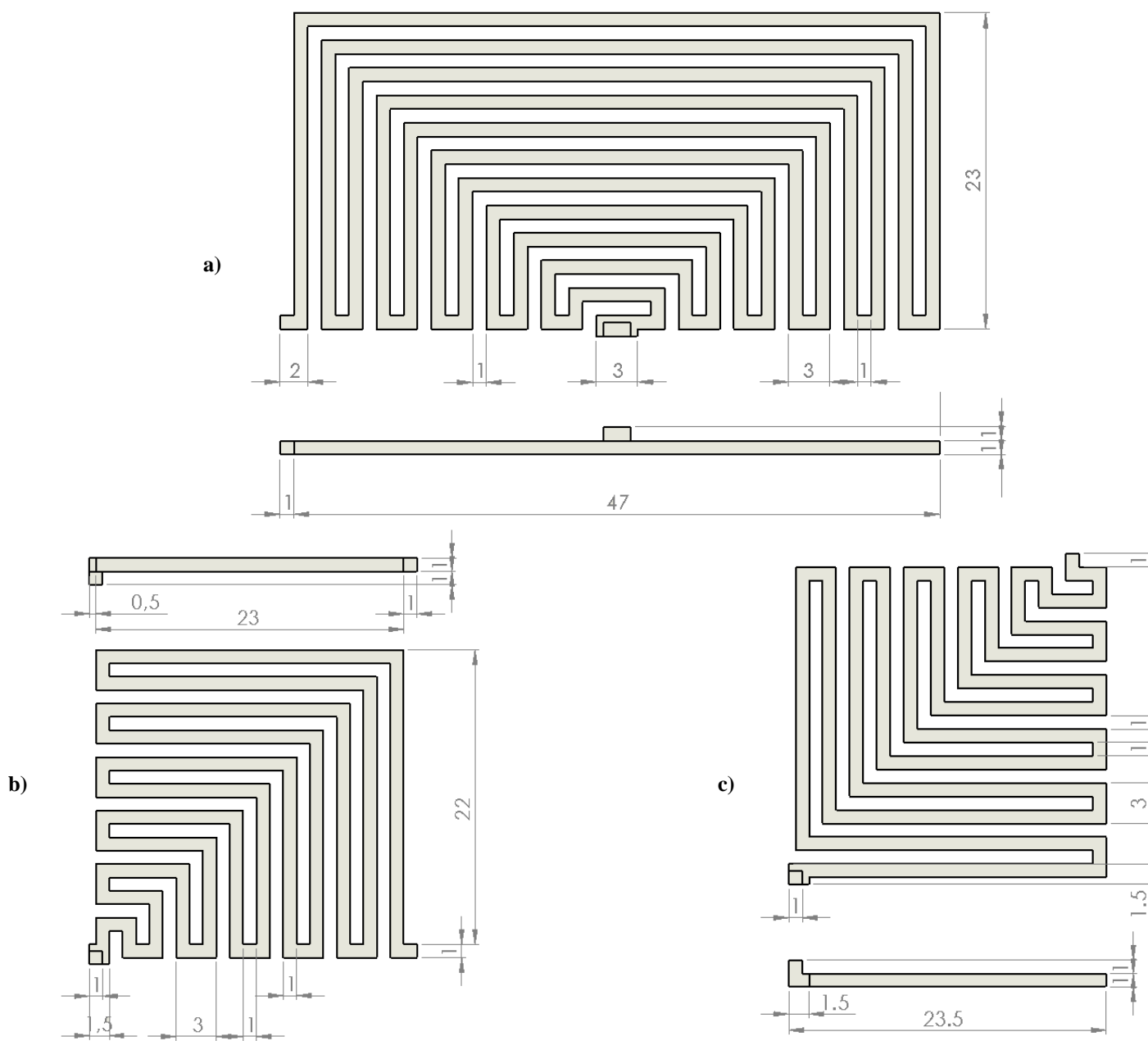**Figure 1.** Schematic of the 3D computational domain.

Figure 2. Different geometries used for the simulations. **a)** D1 configuration **b)** D2-A configuration **c)** D2-B configuration [mm].

Boundary Conditions

The velocity at inlet was fixed for all studied cases with a constant value corresponding to a Reynolds number of Re=521, and an inlet temperature of 300 K. Both inlet temperature and velocity are assigned as boundary conditions in the presented model. Figure 3 shows a schematic representation of the computational and the applied boundary conditions.
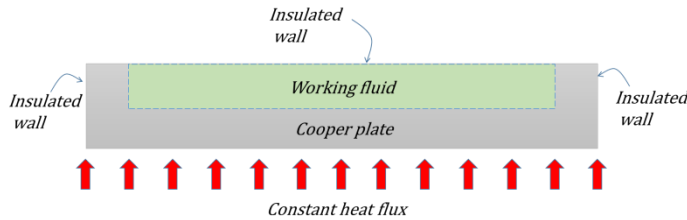

Figure 3. A 2D schematic of the computation domain of a heat sink.

A constant pressure is set as boundary conditions for the outlets of the heat sink. Non-slip condition is stablished for the interface faces. The walls surrounding the heat sink are insulated as shown in Figure 3. A constant heat flux of 100 kW/m^2 is applied to the base of the cooling plate. Constant velocity boundary condition is set to the inlet of the device.

Numerical Procedure

The numerical solution of the governing equations was realized using a computational fluid dynamics (CFD) software ANSYS® Fluent. This software performs the finite volume method and solves the governing equations numerically. For the coupling of the velocity and pressure, the SIMPLE algorithm was selected. Convergence criteria were determined by residuals of the solution. When the mass and momentum conservation residuals reaches a value below 10^{-4} and energy equation below 10^{-7} the solution is considered enough accurate.

Table 3 contains details of the mesh sensibility analysis. Pressure drop and outlet fluid temperature are selected as comparison parameters among the different levels of meshing. The grid independence was achieved by mesh refinements. The number of elements is approximately doubled from one mesh to

other until the criterion $\left|\frac{\Delta P^j - \Delta P^{j+1}}{\Delta P^j}\right| < 1 \times 10^{-2}$ and $\frac{T^j_{f,out} - T^{j+1}_{f,out}}{T^j_{f,out}}$ is attained.

RESULTS AND DISCUSSION

A uniform temperature distribution is one of the main goals of cooling devices. For the three flow pattern proposed, Figure 4 shows the temperature of the heat sink base (surface where the heat flux is applied). Flow pattern D1 presents a good temperature distribution, exhibiting a variation of 2.65 K between the maximum and minimum temperature in the heating surface.

Using the flow pattern D2-B, the bottom of the heat sink has the smaller temperature variation. A bigger surface is covered since the flow is distributed in longer channels by the fluid inlet, cooler water can be distributed along the heat sink and it can help to increase the temperature uniformity and benefits the heat transfer driving force. For this design the long channels are a characteristic way to distribute the fluid along the device.

In the case of designs D1 and D2-Aa the fluid is guided through shorter channels near to the center of the heat sink, then, the fluid cover the exterior part of the heat sink. At this point the fluid has increased its temperature; therefore the heat transfer will be lower in the exterior channels of the flow field due to the decrease of the heat transfer driving force.

The variation of the thermal resistance along a diagonal line at the heating surface is presented in Figure 5 for each configuration. Flow patterns D1 showed the lowest thermal resistance. At the center of the heat sink the thermal resistance is lower due to the position of the flow inlet; in this zone the fluid has a cooler temperature.

Other important fact in liquid cooling heat sinks is the pressure drop. A high pressure drop requires higher pumping power; this power must be supply by an external source. Figure 6 and 7 show the pressure field of the three studied flow patterns. In order to obtain the pressure drop, averages values for pressure were calculated with numerical integration at inlet and outlet. The pressure drop using the flow pattern D1 is 5 times bigger than the presented by D2-A or D2-B designs.

Table 3. *Grid sensitivity analysis for the proposed flow pattern configuration.*

| Flow patter design	Mesh model	Mesh elements	Δp [kPa]	$\left\|\frac{\Delta p^j - \Delta p^{j+1}}{\Delta p^j}\right\|$	$T_{f,out}$ [K]	$\frac{T^j_{f,out} - T^{j+1}_{f,out}}{T^j_{f,out}}$
D1	1	1,041,552	3,358.26	1.053×10^{-1}	303.77	2.1×10^{-3}
	2	2,468,864	3,004.67	2.675×10^{-3}	303.13	9.5×10^{-4}
	3	4,822,000	3,012.71	-	302.84	-
D2a	1	1,041,522	621.27	4.61×10^{-2}	304.69	2.59×10^{-3}
	2	2,468,864	602.64	4.74×10^{-3}	304.00	7.57×10^{-4}
	3	4,822,000	589.83	-	303.67	-
D2b	1	1,041,522	637.09	3.2×10^{-2}	303.96	1.78×10^{-3}
	2	2,468,864	657.48	8.69×10^{-3}	304.50	2.96×10^{-4}
	3	4,822,000	663.181	-	304.41	-
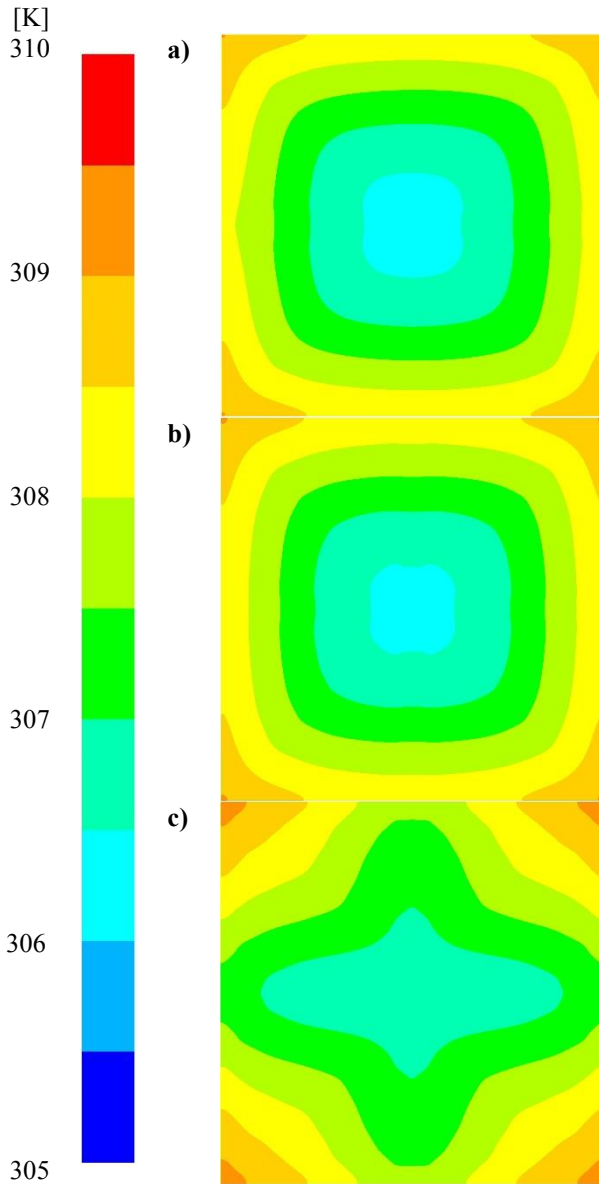
Figure 4. Temperature distribution: a) D1, b) D2-A, c) D2-B.

Table 4 presents a summary of the main characteristic of the heat sinks using different flow pattern configuration. The required pumping power is calculated by Equation 8.

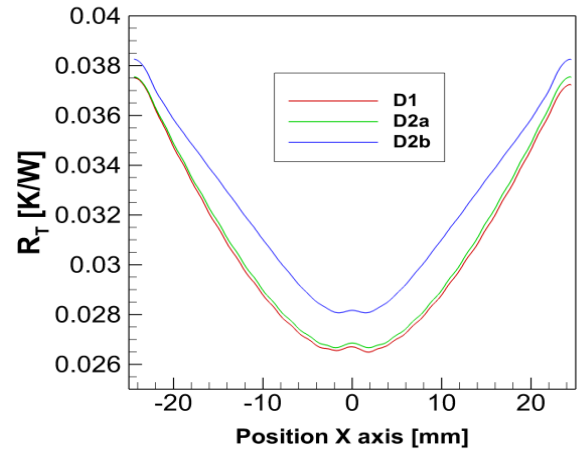$$\dot{W}_P = \Delta p \, \dot{\forall} \qquad (8)$$

Figure 5. Local thermal resistance.

A modified coefficient of performance proposed in [13] is defined by Equation 9.

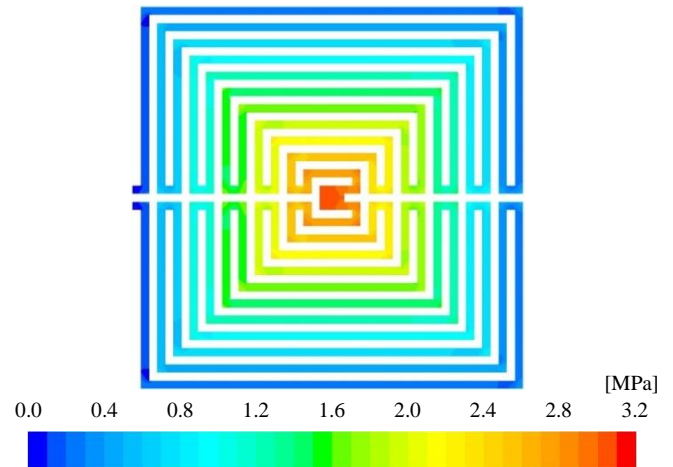$$COP_m = \frac{q''A_s}{\Delta T_s \dot{W}_p} \qquad (9)$$

Figure 6. Pressure field in design D1.

Coefficient of performance relates the amount of energy that can be dissipated from a system with the energy required to remove it. In order to consider the temperature uniformity at the base of the plate, COP_m includes the maximum temperature difference at heating surface. Considering COP_m as a comparison parameter, design D2-A has the best overall performance. This parameter can be seen in Table 4.
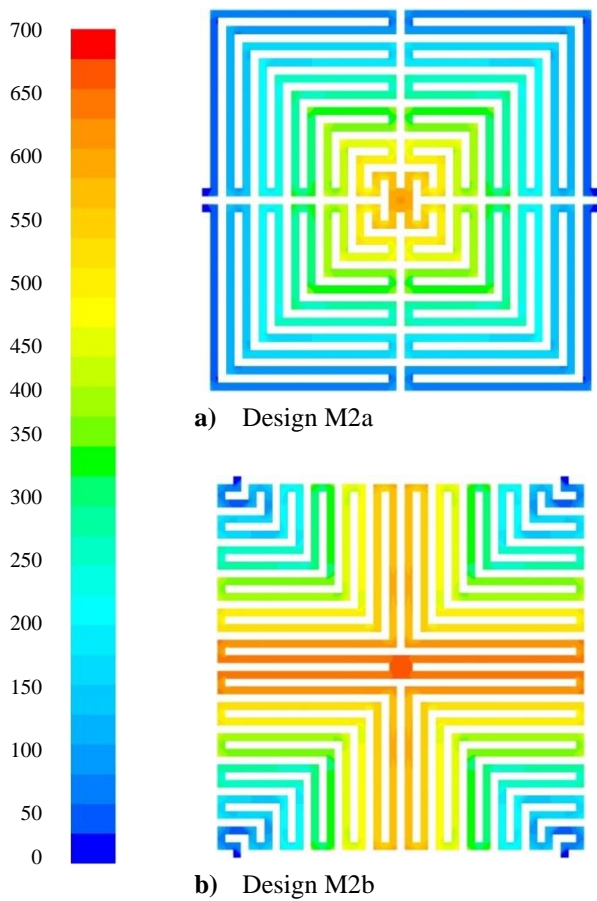
Table 4. *Cooling performance for the different flow configuration*.

Design	$T_{max, b}$ [K]	$T_{min, b}$ [K]	$T_{ave, b}$ [K]	ΔT_b [K]	$R_{T, max}$ [K/W]	Δp (pressure drop) [kPa]	Pumping Power [W]	COP_m
D1	308.99	306.34	307.54	2.65	0.03755	3023.7	69.3	1.31
D2a	309.00	306.39	307.59	2.61	0.03755	589.8	13.6	6.76
D2b	309.17	306.67	307.61	2.50	0.03826	663.2	15.2	6.32

[kPa]

a) Design M2a

b) Design M2b

Figure 7. Pressure fields.

CONCLUSIONS

Liquid cooling is a good alternative for mitigating high temperatures reached in the new generation electronic devices. In the present study a numerical simulation of a heat sink using different flow pattern designs was performed. The temperature distribution at the heating surface was used as a performance comparison parameter. The three designs showed a similar variation of the temperature distribution. The D1 designs demonstrated to be the one that presents the lower base temperature. However, the required pumping power is about 5 times bigger that the required by D2-A and D2-B configurations.

The results indicate that the flow pattern D2-B has the best performance, presenting the lower pumping power requirements, and showing a good temperature distribution. This is described in Table 4 by the highest COP_m obtained. The new COP_m definition is a good comparison parameter for this type of cooling devices; however, there are some factors that are not well described by this simple coefficient. A better defined coefficient considering temperature uniformity must be studied and defined.

The number of channels affects directly the pressure drop of the heat sink. Although the temperature distribution at the base of the heat sink is not strongly changed. Therefore a new flow pattern configuration with a bigger number of channels could decrease the pumping power requirements improving the overall performance of the heat sink.

REFERENCES

[1]   S.G. Kandlikar, High Flux Heat Removal with Microchannels −A Roadmap of Challenges and Opportunities, Heat Transfer Engineering, 26 (8), 2005, Pages 5-14.

[2]   D.B. Tuckerman, R.F.W. Pease, High-performance heat sinking for VLSI, IEEE Electron Devices Lett, EDI-2 (5), 1981, Pages 126-129.

[3]   X.L. Xie, Z.J. Liu, Y.L. He, W.Q. Tao, Numerical study of laminar heat transfer and pressure drop characteristics in a water-cooled minichannel heat sink, Applied Thermal Engineering 29, 2009, Pages 64–74.

[4]   Yongping Chen, Ping Cheng, Heat transfer and pressure drop in fractal tree-like microchannel nets, International Journal of Heat and Mass Transfer 45, 2002, Pages 2643–2648.

[5]   Xiang-Qi Wang, Arun S. Mujumdar , Christopher Yap, Thermal characteristics of tree-shaped microchannel nets for cooling of a rectangular heat sink, International Journal of Thermal Sciences 45, 2006, Pages 1103–1112.

[6]   V.D. Zimparov, A.K. da Silva, A. Bejan, Thermodynamic optimization of tree-shaped flow geometries with constant channel wall temperature, International Journal of Heat and Mass Transfer 49, 2006, Pages 4839–4849.

[7]   L.A.O. Rocha, S. Lorente, A. Bejan, Tree-shaped vascular wall designs for localized intense cooling, Int. Journal. Heat Mass Transf. 52, 2009, Pages 4535–4544.

[8]   Escher, W., Michel, B., Poulikakos, D., Efficiency of optimized bifurcating treelike and parallel microchannel networks in the cooling of electronics. International Journal of Heat and Mass Transfer 52, 2009, Pages 1421–1430.

[9]   Ching-Jenq Ho a, Wei-Chen Chen a, Wei-Mon Yan, Experimental study on cooling performance of minichannel heat sink using water-based MEPCM particles, International Communications in Heat and Mass Transfer 48, 2013, Pages 67–72.

[10]   Saad Ayub Jajja, Wajahat Ali, Hafiz Muhammad Ali, Aysha Maryam Ali, Water cooled minichannel heat sink s for microprocessor cooling: Effect of fi n spacing, Applied Thermal Engineering 64, 2014, Pages 76-82.

[11]   Yu-Tong Mu, Li Chen, Ya-Ling He, Wen-Quan Tao, Numerical study on temperature uniformity in a novel mini-channel heat sink with different flow field configurations, International Journal of Heat and Mass Transfer 85, 2015, Pages 147–157.

[12]   T. Al-Shemmeri, Engineering Fluid Mechanics, Ventus Publishing ApS, London, 2012, Pages 17–18. ISBN 978-87-403-0114-4.

[13]   Daniel Lorenzini-Gutierrez, Satish G. Kandlikar, Variable Fin Density Flow Channels for Effective Cooling and Mitigation of Temperature Nonuniformity in Three-Dimensional Integrated Circuits.